A Study on the Energy Efficiency of Various Gaits for Quadruped Robots: Generation and Evaluation

Roman Zashchitin[a] and Dmitrii Dobriborsci[b]
Deggendorf Institute of Technology, 93413 Cham, Germany

Keywords: Quadrupedal Robots, Walking Robots, Reinforcement Learning, Gait Generating.

Abstract: This paper presents an approach for generating various types of gaits for quadrupedal robots using limb contact sequencing. The aim of this research is to explore the capabilities of reinforcement learning in reproducing and optimizing locomotion patterns. The proposed method utilizes the PPO algorithm, which offers improved performance and ease of implementation. By specifying a sequence of limb contacts with the ground, gaits such as Canter, Half bound, Pace, Rotary gallop, and Trot are generated. The analysis includes evaluating the energy efficiency and stability of the generated gaits. The results demonstrate energy-efficient locomotion patterns and the ability to maintain stability. The findings of this study have significant implications for the practical application of legged robots in various domains, including inspection, construction, elderly care, and home security. Overall, this research showcases the potential of reinforcement learning in gait generation and highlights the importance of energy efficiency and stability in legged robot locomotion.

1 INTRODUCTION

For an extended period of time, starting from the late 20th century, scientific research has been conducted to explore the applicability of Reinforcement Learning (RL) algorithms in the field of multidimensional robot control, including helicopters (Bagnell and Schneider, 2001), (Ng et al., 2003), bipeds (Zhang and Vadakkepat, 2003), and quadrupeds (Hornby et al., 1999). The main advantage of walking robots over wheeled robots is the ability to move on uneven terrain through the use of intermittent contact and the possibility of shifting the center of mass relative to the point of contact, which is provided by leg mechanisms (Kim and Wensing, 2017). All the above-mentioned allows the use of such robots in various areas: inspection, construction, care of the elderly, home security, etc. Even in the early stages of studies, the potential of automated motion generation, where speed is an important success criterion, was demonstrated (Kohl and Stone, 2004).

The problem formulated during that time remains relevant to this day:

- Simplifying multidimensional control and the process of tuning parameterized movements, which currently require significant time and extensive operator experience. Additionally, changes in hardware configuration or surface characteristics also necessitate system recalibration.
- Ensuring more efficient and optimal movements of robotic systems.
- Improving speed, stability, energy efficiency, and adaptability to diverse environmental conditions.
- Creating universal models applicable to different types of robots, eliminating the need to manually adjust gait for each specific robot.

The area of walking robots has made significant progress in recent years, with the development of sophisticated hardware (Hutter et al., 2016) and control algorithms (Hwangbo et al., 2019). However, a major challenge remains in the ability to automatically generate robust and efficient gaits for these robots. This is particularly important for real-world applications, where the robots must navigate unpredictable and complex environments.

In nature, there exists a vast variety of animal gaits, characterized by different tempos, dynamics, and purposes. Each of these gaits possesses its advantages and disadvantages, including high speed and energy efficiency. This paper does not aim to find a universal gait; instead, it employs the principles of

[a] https://orcid.org/0009-0001-7637-5517
[b] https://orcid.org/0000-0002-1091-7459

Zashchitin, R. and Dobriborsci, D.
A Study on the Energy Efficiency of Various Gaits for Quadruped Robots: Generation and Evaluation.
DOI: 10.5220/0012234600003543
In *Proceedings of the 20th International Conference on Informatics in Control, Automation and Robotics (ICINCO 2023) - Volume 1*, pages 311-319
ISBN: 978-989-758-670-5; ISSN: 2184-2809

biomimicry to generate various gaits observed in nature using reinforcement learning. Specifically, the study examines gaits such as Canter, Half bound, Pace, Rotary gallop, and Trot. Following the training of the reinforcement learning algorithm using these reference gaits, an analysis is conducted to assess the energy efficiency of these gaits at different speeds and evaluate the algorithm's learning capability.

Two aspects of legged locomotion are of greater interest in this study: dynamic physical interaction with the environment and energy efficiency. Dynamic locomotion requires more complex control algorithms and is generally more challenging than static locomotion. It is necessary to estimate the state of the robot: the state vector of the system, which includes linear and angular coordinates of the torso, leg positions, rotation joint angles, etc. Then the state vector is transmitted to the control system, which is directly responsible for the coordination of all body parts in space, generates trajectories of tool points in the mechanism, the angle of attack, the generation of moments on the joints, and other indicators responsible for gait and balance. The implementation of such complexly structured and massive control systems is often a costly and time-consuming process, due to the description of the system by complex dependencies.

2 GAIT GENERATION METHOD

2.1 Reinforcement Learning

This paper uses a class of reinforcement learning algorithms PPO (Proximal Policy Optimization) (Schulman et al., 2017b), which provides similar or better performance than current approaches, but has a simpler implementation and tuning. Supervised learning leaves it possible to implement a cost function, use gradient descent, and get good results with relatively little hyperparameter tuning. PPO strikes a balance between simple implementation, sampling complexity, and ease of tuning. The PPO function has the form:

$$L^{CLIP} = \hat{E}_t\Big[\min\Big(r_t(\theta)\hat{A}_t, clip\big(r_t(\theta), 1-\varepsilon, 1+\varepsilon\big)\hat{A}_t\Big)\Big], \quad (1)$$

where θ is the policy parameter, E_t - empirical expectation by time steps, r_t - probability ratio under the new and old policy, A_t - expected time advantage t, ε - hyperparameter.

The PPO-Clip algorithm relies on a specialized clipping mechanism in the objective function to prevent the new policy from deviating too far from the old policy. This approach simplifies the algorithm and makes it compatible with stochastic gradient descent.

The algorithm has been extensively tested and has shown excellent performance in continuous control tasks. By removing the KL-divergence term and the constraint, PPO-Clip streamlines the updating process and provides incentives for the new policy to stay close to the old policy through clipping. (Schulman et al., 2017a).

The goal of reinforcement learning is to learn to act in the environment in the most optimal way possible. The terminology of reinforcement learning and optimal control is thought to be equivalent and tightly overlapping. Optimal action in the environment is achieved by maximizing reward rather than minimizing error.

2.2 Mechanism of Effective Gait

The paper (Bertram and Gutmann, 2009) pays attention to the mechanism of galloping by different animals. It is believed that the main difference between different types of canter is in the set of limbs (hind or forelimbs), which initiate the change of direction of the velocity of the center of mass, during the contact with the ground (Figure 1) (Blickhan, 1989).

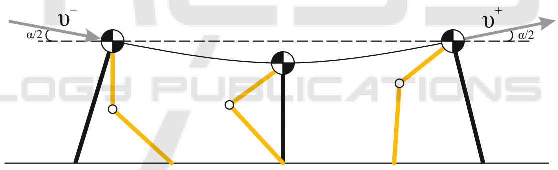

Figure 1: Schematic representation of the transfer of the center of gravity of the leg relative to the point of contact, presented in the paper.

It is during the change of the velocity vector that the greatest loss of momentum and kinetic energy occurs. An important observation is that fast and energy-efficient movement is provided only during dynamic locomotion, when the center of mass is stable for short periods of time. Equation 2 present the dependence of the loss of kinetic energy on the angle of the incoming and outgoing velocity vector.

$$\frac{\Delta E}{E^-} = \sin^2\alpha \approx \alpha^2. \quad (2)$$

Based on equation 2, the fraction of energy lost during the transition from one collision to another is approximately equal to α^2, where α is the angle between the velocity vectors v^- and v^+. This conclusion is valid only for small angles and a single collision.

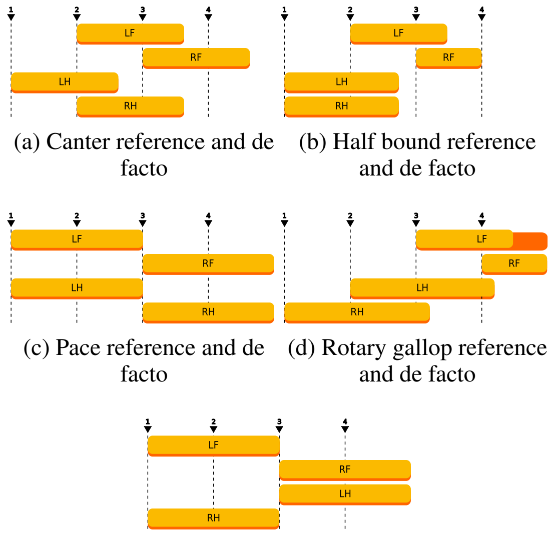

(a) Canter reference and de facto (b) Half bound reference and de facto

(c) Pace reference and de facto (d) Rotary gallop reference and de facto

(e) Trot reference and de facto

Figure 2: Gait diagrams showing coordination patterns for asymmetrical gaits. Shaded bars represent stance phases, open areas between bars represent swing phases, and numbered arrows show footfall timing. The yellow bars show the reference gait and the orange bars show the gait obtained after RL training. LH: left hind limb; RH: right hind limb; LF: left front limb; RF: right front limb.

2.3 Reference Gaits

The book (Clayton, 2004) focuses on biomechanics, dynamics, and various types of gaits, providing a detailed description of aspects such as leg movement sequencing during running, depending on the phase and its cyclic nature.

Initially, one of the primary objectives of this study was to minimize the utilization of mathematical dependencies in gait generation. Consequently, the mathematical description of gait, involving calculations of phase lengths, cycles, cyclic offset angles, and other dependencies, was simplified to the specification of a sequence of limb transitions in contact with the ground. Thus, practically all mathematical dependencies are intended to be addressed by the RL algorithm.

The depicted gaits in the book are illustrated in Figure 2. Detailed explanations regarding the obtained results will be presented in Section 5.

3 ALGORITHM SETTINGS POLICY AND REWARDS

Setting up the environment involves designing a dynamic model of the robot and its environment. A correctly composed model must contain such parameters as:

- Inertia tensors for each link;
- Physical constraints on the motion of links relative to each other, including the collision of objects, for the impossibility of bodies to intersect;
- Physical constraints on the motion of joints, including the range of possible positions, velocities and moments, the value of friction and damping coefficients.

A sufficiently detailed model of ANYmal is provided by the manufacturer in URDF format in the official Github repository, which was taken as a basis (ANYbotics, 2023). The environment at this stage represents a pure plateau with the global damping and friction coefficient set.

Setting up an agent involves making up two vectors of values: a state vector and a control vector. It is important to use only the data that can be obtained with real sensors such as inertial measurement modules, floor contact pressure sensors, position sensors, etc. Thus, the state vector to the agent input consists of a vector of dimension $obDim = 85$, and the output of dimension $actionDim = 12$, equal to the number of motors of the robot. The output vector generates torque values for each robot motor. Other methods of motion control are also possible, such as force control, position control, and velocity-based control.

Computer simulators are physically unable to simulate the real physics of contact interaction and are only approximate (Hwangbo et al., 2018), and machine learning algorithms themselves often find a loophole in the simulator and exploit this inaccuracy. The simulation model of the robot itself, the dynamics, and the coefficient values are also approximate and imply some deviations in the final result of the walking robot. Based on the presented disadvantages of the resulting gait, it becomes necessary to formulate additional rewards.

We have been inspired by the award functions in the papers (Hwangbo et al., 2019), (Lee et al., 2020), (Miki et al., 2022), in developing the functions needed to meet the goals of this paper. The rewards used during training can be divided into several categories that solve a particular problem during gait generation.

In this paper, several experimental rounds are presented, consisting of a combination of soft and hard constraints.

Soft constraints are primarily implemented using reward functions and the assignment of appropriate coefficients. Such constraints on the solution search space allow for gait adaptation to the robot's dynamic characteristics if a specific gait cannot be used without modifications. The algorithm is designed to independently establish dependencies between cycle length, contacts, flight, and phase lengths based on the specified movement speed along the $\hat{x}$ and $\hat{y}$ plane.

To achieve realistic movements and enhance the algorithm's applicability to a physical robot, we introduce rewards that are inversely correlated with metric minimization:

- The error between the actual linear velocity and the given linear velocity command.
- The error between the actual angular velocity command and the given angular velocity command.
- The generated torque of the actuators.
- The speed of the actuators.
- Limb lift relative to the point of contact with the floor and slippage.
- Step changes in speed and torque of the actuators.
- Roll, pitch, and yaw angles of the main body of the robot.
- The robot's center of mass at a certain height.
- The phase time when the limbs are not in contact with the floor.
- The robot's velocity in space along the $\hat{z}$ axis.
- The error in following the reference gait (optional).

Hard constraints serve as an extension to the soft constraints, representing a set of episode interruption functions that are triggered if the robot exceeds the permissible limits during a specified time. For instance:

- Interrupting the episode if contact between the robot and the ground was not made by the robot's leg;
- Interrupting the episode if the robot's body geometric center excessively deviates along the z-axis, relative to the specified position;
- Interrupting the episode if the robot's body yaw deviates excessively from the zero value while running in a straight line;
- Interrupting the episode if the robot's coordinates reach manually set, non-recommended values while running in a straight line.

Hard constraints are imposed to significantly reduce the search space, consequently decreasing the training time. However, with hard constraints in place, the debugging time for reward functions increases, as the training convergence time is noticeably extended.

3.1 Hyperparameters for PPO

The tuning of hyperparameters in the PPO algorithm for reinforcement learning is an essential part of the training process. Hyperparameters, such as learning rate, minibatch size, and the number of optimization epochs, determine various aspects of the algorithm. Making the right choices for these hyperparameters can enhance the performance and efficiency of the algorithm, ensuring faster and more stable convergence towards an optimal policy. However, determining the optimal values for hyperparameters requires experimentation and thorough investigation. Achieving this optimization can significantly impact the algorithm's effectiveness and contribute to the advancement of reinforcement learning techniques (Godbole et al., 2023). The parameters used in the training are presented in Table 1.

Table 1: Hyperparameters for PPO.

	Value
learning rate	5e-4
discount factor	0.998
learning epoch	4
GAE-lambda	0.95
clip ratio	0.2
entropy coefficient	0.0
batch size	4

3.2 Logistic Kernel

We use a logistic kernel to define a bounded cost function. This kernel converts a tracking error to a bounded reward. The logistic kernel ensures that the cost is lower-bounded by zero and termination becomes less favorable.

$Logistic\ Kernel(LK) : \mathbb{R} \to [-0.25, 0)$ as

$$LK(x) = \frac{-1}{\exp^{x} + 2 + \exp^{-x}} \tag{3}$$

3.3 Reward Functions

The process of tuning reward functions in reinforcement learning for robotic systems was carried out in a systematic and iterative manner. Initially, a small number of rewards and their corresponding adjustments were considered. As the process advanced, more sophisticated functions were incorporated to enhance the performance of the robotic system, and these changes were reinforced through multiple rounds of experimentation. These experiments served to verify the functionality of the system and tackle a variety of challenges, such as RL algorithm attempts to exploit vulnerabilities in the simulator's physical engine, unrealistic robot movements, among other issues.

The dynamic locomotion of a complex robotic system featuring 12 degrees of freedom presents a vast and intricate space of potential configurations. Due to the enormity of this space, searching for feasible gaits in all possible configurations is not a practical approach. To optimize the system's performance, it is essential to strike a balance between an excessive search space and an insufficient one. It is possible that the optimal policy for the task at hand may not have been identified within 25,000 epochs. However, the primary experimental trends can often be observed, providing valuable insights into the system's behavior and potential improvements.

To further refine the search process, randomly generated initial points within the search space can be mitigated by increasing the number of trial rounds and training iterations. Interestingly, the best checkpoint is not always the final one in the training process. In this study, we actively monitor and track the best checkpoints observed during the course of training.

Upon completion of the training process, the selection of the most suitable model involves identifying the optimal checkpoint observed during the training. This strategy, known as retrospective optimal checkpoint selection, allows for a more robust and efficient choice, ultimately enhancing the performance and capabilities of the robotic system.

The reward function is defined as:

$$r_{final} = 130 r_{bv} + r_{bw} - 10(r_{j\tau} + r_{jv}) - 100(r_{fc} + r_{fs}) - \\ - 0.1 r_s - 1000 r_{bo} + 0.2 r_{at} - 0.1 r_{za} + 0.5 r_{gg}. \quad (4)$$

The individual terms are defined as follows.

- Linear Velocity (r_{bv}): This term encourages the policy to follow a desired horizontal velocity (velocity in $\hat{x}$ and $\hat{y}$ plane) command:

$$r_{bv} = c_{v1} LK(|c_{v2} \cdot (v^{fact} - v^{des})|), \quad (5)$$

where $c_{v1} = -10\Delta t$, $c_{v2} = -4\Delta t$, $v = [v_x, v_y, v_z]^T$.

- Angular Velocity ($r_{b\omega}$): This term encourages the policy to follow a desired yaw velocity command:

$$r_{b\omega} = c_\omega LK(|w^{fact} - w^{des}|), \quad (6)$$

where $c_\omega = -6\Delta t$, $w = [w_x, w_y, w_z]^T$.

- Joint Torque ($r_{j\tau}$): We penalize the joint torques to reduce energy consumption:

$$r_{j\tau} = c_\tau \sum_{i=1}^{12} \tau_i^2, \quad (7)$$

where $c_\tau = 0.0005\Delta t$.

- Joint Speed (r_{jv}): We penalize the joint speed to reduce jerks and add smoothness to the robot's movements:

$$r_{jv} = c_{vj} \sum_{i=1}^{12} v_{j_i}^2, \quad (8)$$

where $c_{vj} = 0.003\Delta t$.

- Foot Clearance (r_{fc}): We penalize the foot in the swing phase for raising the foot too high:

$$r_{fc} = c_{fcc} \sum_{i=1}^{4} \left((p_{f,i}^{des} - p_{f,i}^{fact})^2 - v_{f,i}^2 \right), \quad (9)$$

where $c_{fcc} = 0.1\Delta t$.

- Foot Slip (r_{fs}): We penalize the foot velocity if the foot is in contact with the ground to reduce slippage:

$$r_{fs} = c_{vf} \sum_{i=1}^{4} v_{f,i}^2, \quad (10)$$

where $c_{vf} = 2.0\Delta t$.

- Smoothness (r_s): We penalize sudden changes in speed and torque on the actuators, to reduce vibration and maintain realism of movement:

$$r_s = c_{sc} \sum_{i=1}^{12} ((\tau_{i,t} - \tau_{i,t-1})^2 + (v_{i,t} - v_{i,t-1})^2), \quad (11)$$

where $c_{sc} = 0.04\Delta t$.

- Body Orientation (r_{bo}): We penalize for deviations of pitch and roll of the robot body from zero values and deviations of the body center height from the set value:

$$r_{bo} = c_{boc} \left(\theta_x + \theta_y + (p_{b,z}^{fact} - p_{b,z}^{des})^2 \right), \quad (12)$$

where $c_{boc} = 0.04\Delta t$.

- Air Time (r_{at}): We reward the agent with a long swing phase, but impose a penalty if the swing phase is too long to avoid excluding the limbs from the gait:

$$r_{at} = \\ = \begin{cases} c_{atc} \sum_{i=1}^{4} \left((t_{f,i} - 0.5) - \exp^{t_{f,i}} \right), & if\ t_{f,i} > 1.5 \\ c_{atc} \sum_{i=1}^{4} (t_{f,i} - 0.5), & if\ t_{f,i} \leq 1.5 \end{cases} \quad (13)$$

where $c_{atc} = 2.0\Delta t$.

- Body z Acceleration (r_{za}): We penalize the acceleration of the robot's body along the z-axis:

$$r_{za} = \frac{v_{bz,t} - v_{bz,t-1}}{\Delta t}. \tag{14}$$

- Gait Generation (r_{gg}): We award an agent for Compliance with reference sets of consistent limb-to-ground contacts:

$$r_{gg} = \begin{cases} 1, & if\ \mathbf{C}_f^{fact} = \mathbf{C}_f^{des} \\ 0, & \text{otherwise.} \end{cases} \tag{15}$$

3.4 Abort Functions

- Wrong contact [1, 2, 3]:

$$\begin{cases} True, & if\ \mathbf{C}_{ground,t} \in \mathbf{C}_{foot} \\ False, & \text{otherwise,} \end{cases} \tag{16}$$

where $\mathbf{C}_{ground,t}$ - set of objects in contact with the surface at a given moment in time, $\mathbf{C}_{foot}$ - set of objects that are allowed to interact with the floor surface.

- Exceeding height [1, 2, 3]:

$$\begin{cases} True, & if\ p_{b,z}^{init} - 0.2 < p_{b,z}^{fact} < p_{b,z}^{init} + 0.1 \\ False, & \text{otherwise.} \end{cases} \tag{17}$$

- Exceeding yaw [1, 3]:

$$\begin{cases} True, & if\ |\theta_z| < 60° \\ False, & \text{otherwise.} \end{cases} \tag{18}$$

- Exceeding yaw [2]:

$$\begin{cases} True, & if\ |\theta_z| < 40° \\ False, & \text{otherwise.} \end{cases} \tag{19}$$

- Exceeding x and y coordinates [2]:

$$\begin{cases} True, & if\ p_{b,x} < -0.3\ or\ |p_{b,y}| > 0.1 \\ False, & \text{otherwise.} \end{cases} \tag{20}$$

4 ENERGY EFFICIENCY CRITERIA

It is common to measure the Cost of Transport (CoT) coefficients to study legged robots' energy-efficiency. CoT is a coefficient that quantifies the energy-efficiency of the movement of animals, humans, or robots

$$CoT = \frac{E}{mgd}, \tag{21}$$

where E is the energy required to transfer a body with mass m over a distance d, and g is the gravity constant. The smallest CoT means the most energy-efficient motion.

To measure the energy consumed by robots during movement, the energy measurement method for actuators was used (Folkertsma et al., 2018). This method is necessary to measure the amount of energy supplied by the actuators to the system, i.e., the entire structure robot.

By this method, it is possible to accurately estimate the energy supplied by the controller to the motors if two conditions are satisfied: first, the actuator force is constant during each moment of time, and second, the position sensor is aligned with the actuator.

When these conditions are satisfied, it is possible to calculate the energy arriving at each moment of time (Zashchitin et al., 2020) in the system, where the energy in the system is equal to the internal product of the force by the difference of discrete positions:

$$\begin{aligned} E = \int_{t_i}^{t_{i+1}} P(t)dt = \int_{t_i}^{t_{i+1}} \langle F(t), v(t) \rangle dt = \\ = \langle F(t_i), q(t_i+1) - q(t_i) \rangle, \end{aligned} \tag{22}$$

where $P(t)$ the supplied power, $F(t)$ and $v(t) = \dot{q}(t)$ the motor force and velocity, respectively, and $q(t_i)$ the motor position at time step t_i. Writing the discrete-time equations in computable form, since eq. 22 needs a motor position from a future time step, where $\bar{F}_{i-1}$ is the control; force set at t_{i-1} and held constant until t_i. The energy estimate in the system can be calculated using the equation:

$$\hat{E}_i = \hat{E}_{i-1} + \bar{F}_{i-1}(q_i - q_{i-1}). \tag{23}$$

in which $\hat{E}_i$ is the energy estimate at time t_i.

5 RESULTS

The duration of each test run lasts 10 seconds. The trained models are run step by step with the given command(horizontal x and y velocity, yawrate) {3, 0, 0}, {2, 0, 0}, {1, 0, 0} and measuring CoT. The results of CoT measurements of policies with soft constraints are shown in the Table 2. It can be seen that with successful simulation completions, the CoT values come quite close to the value of 1.2, which is the

[1] This interrupt function is used when teaching with soft constraints.

[2] This interrupt function is used when teaching with hard constraints.

[3] This interrupt function is used in the final CoT measurements.

reference (He and Gao, 2020). Despite the stability and convergence of the policies, the final testing demonstrates instability of the gaits and outliers in almost half of the cases.

A set of RL plots with a soft set of constraints is shown in Figure 3. Based on the graphs we can note the stability, the trend of how well the agent learns and converges to the optimal policy. Here we can argue that the last control point is one of the most optimal policies.

A set of RL plots with a hard set of constraints is shown in Figure 4. It is noticeable that the convergence of learning is faster, but is unstable. The judgement here is valid that the best control point is not always the end point in the learning process.

Upon completion of the training process, the selection of the most suitable model involves identifying the optimal checkpoint observed during the training. This strategy, known as retrospective optimal checkpoint selection, allows for a more robust and efficient choice, ultimately enhancing the performance and capabilities of the robotic system. Table 3 shows the CoT values of policies trained with hard constraints. It is evident from this series of experiments that nearly all iterations were executed successfully; however, the corresponding CoT values were found to be elevated, indicating reduced energy efficiency. It is plausible that the application of a subsequent round of supplementary training, akin to the methodologies employed in (Bengio et al., 2009) and (Hwangbo et al., 2019), will likely rectify this issue and yield a more precise optimization.

Returning to the topic of gaits Section 2.3, it can be noted that if the reference gait is not specified, the policy defaults to a trot gait 2(e) in the case of soft constraints or a canter gait 2(a) in the case of hard constraints, or it resorts to a gait that utilizes inaccuracies in the physical modeling of the mechanism. As mentioned before, the RL algorithm will strive to replicate the given reference gaits or adapt them to suit its own construction peculiarities like in 2(d). In other cases, the gaits were formed correctly.

To reproduce and review the results, please follow the link provided (Zashchitin and Dobriborsci, 2023).

6 CONCLUSIONS

In this work, we have presented an approach for generating various types of gaits for quadrupedal robots by specifying a sequence of limb contacts with the ground. The study has demonstrated the capability to generate gaits such as Canter, Half bound, Pace, Rotary gallop, and Trot. The proposed method, utilizing the RL algorithm PPO, offers improved performance with simpler implementation and setup. The introduced reward functions simplify, expedite, and automate the process of generating different types of gaits, including energy-efficient and high-speed gaits.

Table 2: CoT of different robot gaits depending on the given command under soft constraints. Green cells in the table indicate successful completion of the simulation without exceeding the permissible values. Conversely, orange cells mean unsuccessful completion of the simulation with exceeding the permissible values.

Command	{3, 0, 0}	{2, 0, 0}	{1, 0, 0}
	CoT		
Canter	1.35	1.41	1.55
Half bound	1.40	1.48	1.61
Pace	1.42	1.47	1.57
Rotary gallop	1.42	1.46	1.57
Trot	1.36	1.36	1.41
Without gait reference	1.18	1.24	1.41

Table 3: CoT of different robot gaits depending on the given command under hard constraints. Green cells in the table indicate successful completion of the simulation without exceeding the permissible values. Conversely, orange cells mean unsuccessful completion of the simulation with exceeding the permissible values.

Command	{3, 0, 0}	{2, 0, 0}	{1, 0, 0}
	CoT		
Canter	1.49	1.5	1.55
Half bound	1.41	1.47	1.62
Pace	1.61	1.58	1.63
Rotary gallop	1.48	1.5	1.65
Trot	1.5	1.49	1.60
Without gait reference	1.46	1.47	1.60

After generating the gaits, an analysis was conducted to evaluate their energy efficiency and stability. The assessment of energy efficiency demonstrated that the proposed method achieves energy-efficient gaits, contributing to the optimization of robotic locomotion in terms of power consumption and overall energy expenditure. Additionally, the stability analysis revealed that the obtained gaits exhibit robustness and reliability, maintaining their desired patterns.

The results have shown the stability of the proposed method even with a small number of epochs, making it suitable for real-world deployment on legged robot platforms. These findings highlight the potential of the approach in various applications, such as inspection, construction, elderly care, and home security.

Overall, our approach provides valuable insights into gait generation for legged robots, showcasing the

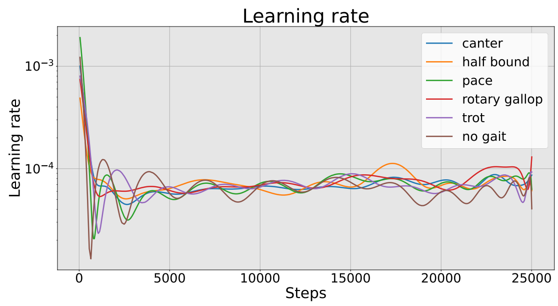

(a) Graph of the dependence of the logarithm of the learning rate on the number of epochs.

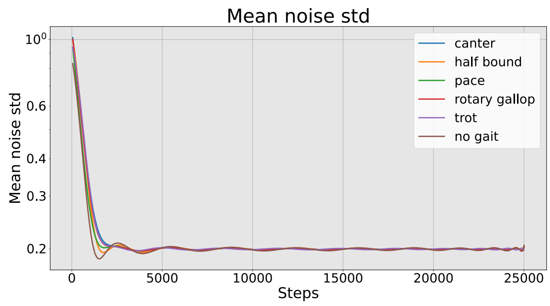

(b) Graph of the dependence of the logarithm of the mean standard deviation of noise on the number of epochs.

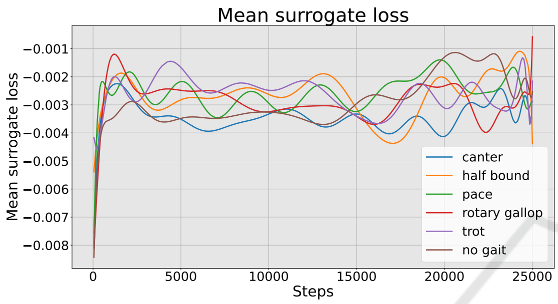

(c) Graph of the surrogate loss function dependence on the number of epochs.

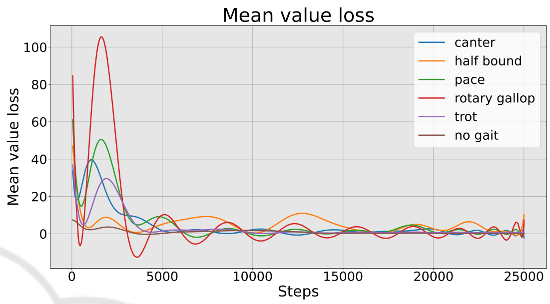

(d) Graph of the value function estimation dependence during training on the number of epochs.

Figure 3: An overview of the key metrics of the reinforcement learning process in the PPO algorithm with soft constraints.

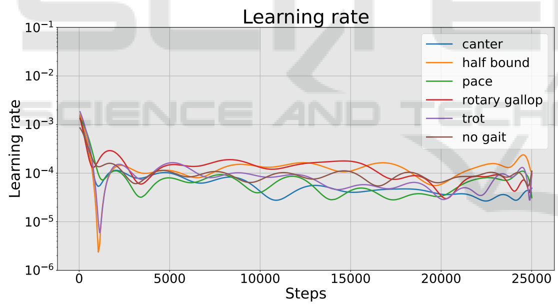

(a) Graph of the dependence of the logarithm of the learning rate on the number of epochs.

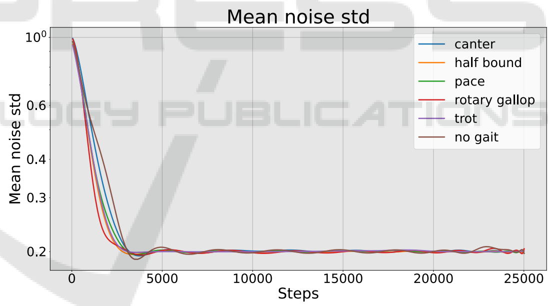

(b) Graph of the dependence of the logarithm of the mean standard deviation of noise on the number of epochs.

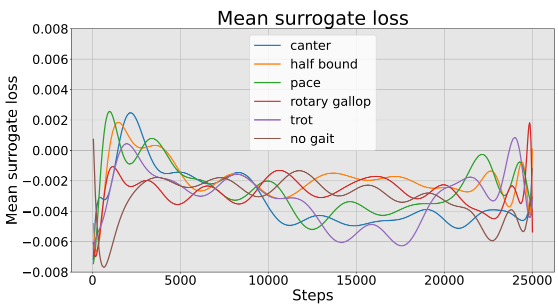

(c) Graph of the surrogate loss function dependence on the number of epochs.

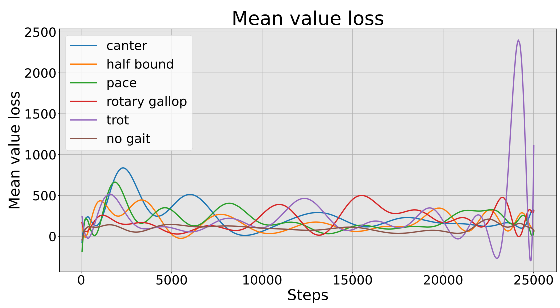

(d) Graph of the value function estimation dependence during training on the number of epochs.

Figure 4: An overview of the key metrics of the reinforcement learning process in the PPO algorithm with hard constraints.

ability to generate stable, energy-efficient, and versatile gaits. By combining reinforcement learning and limb contact sequencing, we have demonstrated the applicability of legged robots in diverse scenarios. The analysis of energy efficiency and stability further reinforces the significance of this approach and its potential for practical implementation. Future research may focus on optimizing gait patterns, incorporating dynamic environments, and considering robustness to varying terrains, thereby expanding the capabilities and applications of legged robots.

REFERENCES

ANYbotics (2023). ANYmal - Autonomous Legged Robot GitHub. https://github.com/ANYbotics.

Bagnell, J. and Schneider, J. (2001). Autonomous helicopter control using reinforcement learning policy search methods. *International Conference on Robotics and Automation*.

Bengio, Y., Louradour, J., Collobert, R., and Weston, J. (2009). Curriculum learning. In *Proceedings of the 26th Annual International Conference on Machine Learning*, ICML '09, page 41–48, New York, NY, USA. Association for Computing Machinery.

Bertram, J. E. and Gutmann, A. (2009). Motions of the running horse and cheetah revisited: Fundamental mechanics of the transverse and rotary gallop. *Journal of the Royal Society Interface*, 6(35):549–559.

Blickhan, R. (1989). The spring-mass model for running and hopping. *Journal of biomechanics*, 22 11-12:1217–27.

Clayton, H. (2004). *The Dynamic Horse A Biomechanical Guide to Equine Movement and Performance*. Sport Horse Publications.

Folkertsma, G. A., Groothuis, S. S., and Stramigioli, S. (2018). Safety and guaranteed stability through embedded energy-aware actuators. In *2018 IEEE International Conference on Robotics and Automation (ICRA)*, pages 2902–2908.

Godbole, V., Dahl, G. E., Gilmer, J., Shallue, C. J., and Nado, Z. (2023). Deep learning tuning playbook. Version 1.0.

He, J. and Gao, F. (2020). Mechanism, actuation, perception, and control of highly dynamic multilegged robots. *Chinese Journal of Mechanical Engineering (English Edition)*, 33.

Hornby, G. S., Fujita, M., Takamura, S., Yamamoto, T., and Hanagata, O. (1999). Autonomous evolution of gaits with the sony quadruped robot. In *Proceedings of the 1st Annual Conference on Genetic and Evolutionary Computation - Volume 2*, GECCO'99, page 1297–1304, San Francisco, CA, USA. Morgan Kaufmann Publishers Inc.

Hutter, M., Gehring, C., Jud, D., Lauber, A., Bellicoso, C. D., Tsounis, V., Hwangbo, J., Bodie, K., Fankhauser, P., Bloesch, M., Diethelm, R., Bachmann, S., Melzer, A., and Hoepflinger, M. (2016). Anymal - a highly mobile and dynamic quadrupedal robot. In *2016 IEEE/RSJ International Conference on Intelligent Robots and Systems (IROS)*, pages 38–44.

Hwangbo, J., Lee, J., Dosovitskiy, A., Bellicoso, D., Tsounis, V., Koltun, V., and Hutter, M. (2019). Learning agile and dynamic motor skills for legged robots. *Science Robotics*, 4(26):eaau5872.

Hwangbo, J., Lee, J., and Hutter, M. (2018). Per-contact iteration method for solving contact dynamics. *IEEE Robotics and Automation Letters*, 3(2):895–902.

Kim, S. and Wensing, P. M. (2017). Design of Dynamic Legged Robots. *Foundations and Trends in Robotics*, 5(2):117–190.

Kohl, N. and Stone, P. (2004). Policy gradient reinforcement learning for fast quadrupedal locomotion. In *IEEE International Conference on Robotics and Automation, 2004. Proceedings. ICRA '04. 2004*, volume 3, pages 2619–2624 Vol.3.

Lee, J., Hwangbo, J., Wellhausen, L., Koltun, V., and Hutter, M. (2020). Learning quadrupedal locomotion over challenging terrain. *CoRR*, abs/2010.11251.

Miki, T., Lee, J., Hwangbo, J., Wellhausen, L., Koltun, V., and Hutter, M. (2022). Learning robust perceptive locomotion for quadrupedal robots in the wild. *Science Robotics*, 7(62):eabk2822.

Ng, A., Kim, H. J., Jordan, M., and Sastry, S. (2003). Autonomous helicopter flight via reinforcement learning. *Advances in Neural Information Processing Systems 17*.

Schulman, J., Klimov, O., Wolski, F., Dhariwal, P., and Radford, A. (2017a). Proximal Policy Optimization.

Schulman, J., Wolski, F., Dhariwal, P., Radford, A., and Klimov, O. (2017b). Proximal policy optimization algorithms. *CoRR*, abs/1707.06347.

Zashchitin, R. and Dobriborsci, D. (2023). GaitGeneration2023. https://github.com/thd-research/code-2023-study-quadruped-gait. Accessed: 2023-07-01.

Zashchitin, R. A., Borisov, I. I., Borisova, O. V., and Kolyubin, S. A. (2020). Energy-efficiency in legged robots locomotion: Open versus closed chains. In *2020 International Conference Nonlinearity, Information and Robotics (NIR)*, pages 1–6.

Zhang, R. and Vadakkepat, P. (2003). An evolutionary algorithm for trajectory based gait generation of biped robot. *Proceedings of the International Conference on Computational Intelligence, Robotics and Autonomous Systems*.